Integration of multicomponent time-lapse processing and interpretation: Focus on shear-wave splitting analysis

Jeff P. Grossman and Gulia Popov, Sensor Geophysical
Chris Steinhoff, Colorado School of Mines

Multicomponent seismic processing and interpretation have become disconnected in industry practice, hindering the ability to extract meaningful reservoir characterization conclusions. Integrating seismic processing with the final interpretation goals elevates the overall characterization that can be performed, and drives advancements in processing algorithms. The focus of this study is on converted-waves because of their high sensitivity to the azimuthal anisotropy caused by preferential fractures and differential stress, and ultimately because they provide a method of correlating hydraulic stimulation success to the enhanced permeability pathways created in the hydraulic completion process.

This study combines the processing and interpretation of the Pouce Coupe time-lapse multicomponent surveys (Figure 1), investigating two horizontal well hydraulic stimulations of the Montney shale. The processing was greatly improved over previous unsatisfactory results by deploying new methods to better preserve vector fidelity, improve prestack shear-wave splitting analysis and layer stripping, and enhance time-lapse repeatability. The results show a strong correlation between the magnitude and orientation of seismically derived induced reservoir azimuthal anisotropy and individual stage production. The baseline characterization provides a strong argument that drilling and completion practices must be driven by the interpretation of the local scale reservoir complexities that will improve completion success.

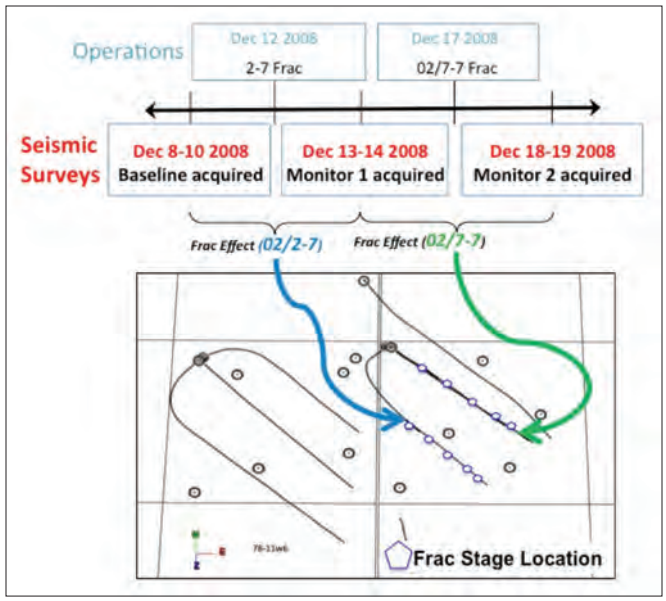

Figure 1. *Pouce Coupe Field operations and 3C-4D multicomponent time-lapse seismic time line. The seismic data consist of a baseline survey and two monitoring surveys of the horizontal well "frac" treatments. Modified from Atkinson and Davis (2011).*

Introduction

The Pouce Coupe time-lapse multicomponent data provide insight into stress and fracture-related reservoir shear-wave anisotropy through the analysis of shear-wave splitting. Atkinson and Davis (2011) found promising results relating to shear-wave seismic anisotropy changes within the Montney shale unconventional reservoir when they analyzed the Pouce Coupe multicomponent time-lapse seismic surveys. It was also concluded that the previous seismic processing was inadequate and required technical improvements in order to extract meaningful reservoir characterization solutions.

In response, the data have been reprocessed, and this study outlines the developments that have been made since then on integrative methods of processing and interpretation as a consequence of focusing our objective on azimuthal anisotropy mapping. Specifically, on the processing side, we discuss receiver azimuth detection and rotation (RADAR), simultaneous nrms (normalized root mean squared)-guided processing, and maximization of coherence of the radial component for shear-wave splitting analysis of common azimuth stacks.

Interpretation of the azimuthal anisotropy within the reservoir interval was determined poststack using shear-wave velocity anisotropy (SWVA), quantified by the time delays between the fast shear and slow shear traveltimes of the base of the reservoir event (Martin and Davis, 1987). The baseline was interpreted for in-situ reservoir conditions and two hydraulic fracture stimulations were monitored to determine the induced azimuthal anisotropy. The azimuthal anisotropy responses were then linked to production log data characterizing the contribution of flow from individual stage locations.

Processing

Certain important multicomponent processing and quality control algorithms such as shear-wave splitting analysis and layer stripping, which we discuss later in this article, tacitly rely on the vector fidelity of the recording to be maintained and for this reason have often failed to provide reliable results. Fundamental improvements to processing methods such as those we present in this paper allow for more sophisticated algorithms to be deployed, and thus for additional information to be accurately extracted from seismic data.

RADAR. RADAR is a recently developed high-fidelity method for automatically detecting and correcting receiver azimuths (Grossman and Couzens, 2012). It addresses vector fidelity problems—ultimately caused by errors in the recorded receiver azimuth—which arise during rotation of the laterally polarized data measurements from the acquisition coordinates into orthogonal radial and transverse coordinates

(Gaiser, 1999). Such errors can and do arise in practice, causing undesirable "leakage" of radial energy onto the transverse component. This in turn can easily be misinterpreted either as evidence of shear-wave splitting (Cary, 2002) or out-of-plane reflection energy.

The impact of this analysis on the Pouce Coupe converted-wave data is illustrated by the reduction of coherent energy on the transverse component, with and without RADAR in Figure 2. All four receiver gathers are transverse component data, where each column corresponds to a different receiver station location. The bottom row shows a large amount of transverse energy after rotation to the reported azimuth, and the top row shows the reduced transverse energy after RADAR. Energy from shear-mode head waves is also evident in the lower left-hand corner of both results. Again as desired, this erroneously transverse-oriented energy is weaker and much less coherent in the RADAR results.

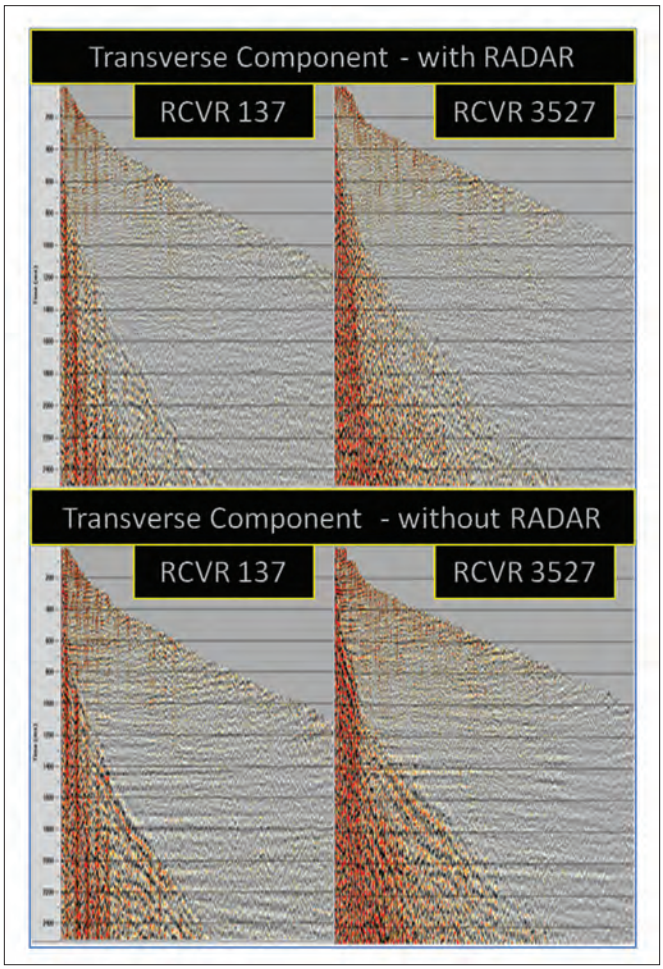

Figure 2. *Transverse-component receiver gathers at two locations (one per column), transformed from field coordinates using two different rotation angles: (1) the RADAR-detected azimuth (top row) and (2) the reported azimuth (bottom row). The improved reduction of energy for the RADAR result indicates an improvement in vector fidelity, as coherent energy is normally not expected to appear on the transverse component. The remarkable coherence change of the shear refracted energy (the dipping events on the bottom left corner of each panel) is more diagnostic than the general changes in reflection energy because it is generated closer to the surface and is therefore less subject to influences from inhomogeneities or anisotropy at depth.*

Additional evidence in support of RADAR is provided by careful examination of the common receiver stacks depicted in Figure 3. Radial and transverse component receiver stacks are shown, with and without RADAR applied, for the baseline and both monitors. The improvement in vector fidelity achieved by applying RADAR is evident from the fact that energy has visibly moved from the transverse component onto the radial component, and in such a way that the lateral coherence on the radial component is enhanced. As we will see later in this paper, the mildly coherent energy remaining on the transverse component stacks is caused by shear-wave splitting.

The successful rotation of the raw data into radial and transverse (R and T) coordinates using the correct azimuth led to many improvements in the processing of the Pouce Coupe multicomponent data set, including the shear-wave splitting analysis and layer stripping results, and more generally with regard to enhanced repeatability across the baseline and both monitors. Repeatability was also enhanced by incorporating

Figure 3. *Common receiver stacks along a fixed receiver line for all three vintages (rows), with and without RADAR applied (right and left columns, respectively). Radial and transverse component stacks are both shown (left and right subcolumns) for each vintage with and without RADAR applied. The improvement in vector fidelity achieved by applying RADAR is evident from the fact that energy has moved from the transverse component onto the radial component in such a way that the lateral coherence on the radial component is enhanced. The somewhat coherent remaining energy on the transverse component stacks is caused by shear-wave splitting.*

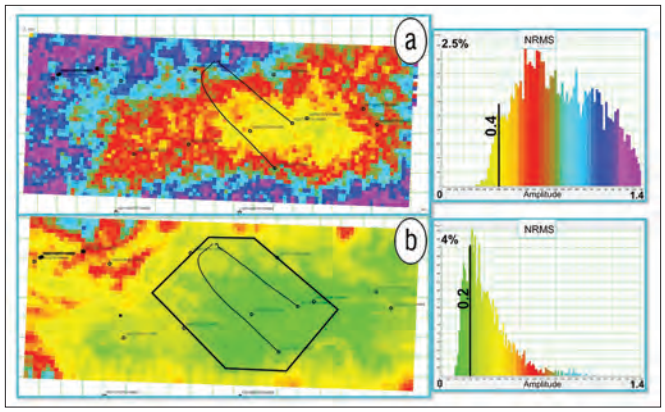

Figure 4. *Normalized root mean square error (Monitor 1–Baseline) histograms and maps corresponding to final processing product with (b) and without (a) RADAR preprocessing applied. The overall improvement in repeatability is evidenced by the lower mean and variance in the distribution of nrms error values. The data analysis polygon is outlined on (b) and was chosen based on the high repeatability zone above the well locations.*

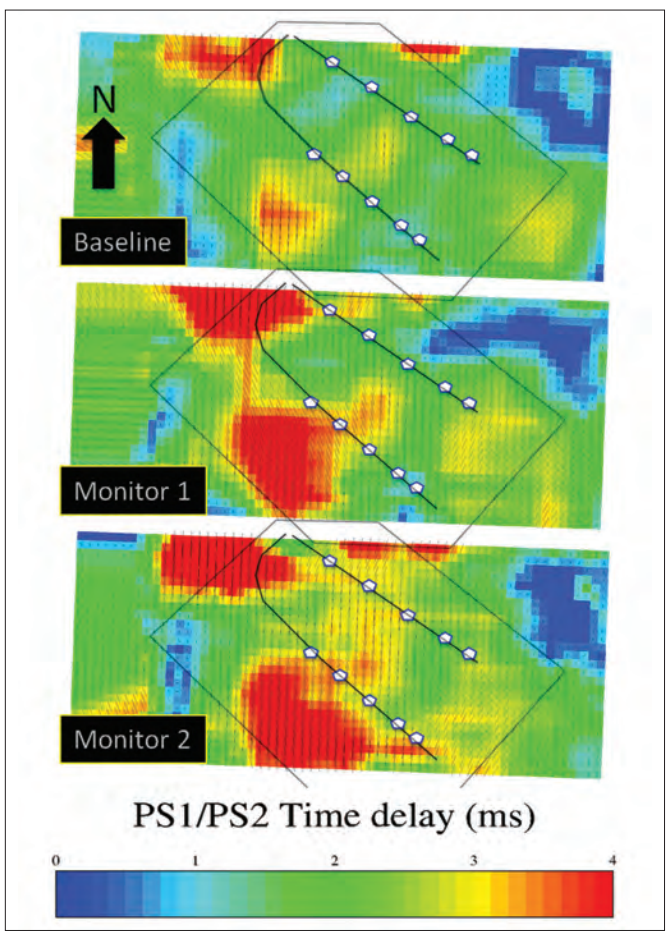

Figure 5. *Prestack time-delay and PS1 azimuth estimates resulting from the layer-stripping procedure down to the reservoir level, displayed for all three vintages of the Pouce Coupe time-lapse seismic survey. The polygon drawn on each map bounds the area of interest for this study, and the wells are drawn along with hydraulic fracture stages indicated by the small pentagons. The color scale represents the estimated time delays between PS1 and PS2 events while the needle length and orientation represent the estimated PS1 azimuths. As explained in the interpretation section, gradual background increases in time delay are directly associated with reservoir activity. Changes in orientation are negligible.*

the simultaneous nrms-guided time-lapse processing methodology of Li et al. (2012), which we explain next.

Time-lapse processing. The complete Pouce Coupe multicomponent data set was processed for the highest repeatability, which allows for any time-lapse effects to be interpreted as physical changes in the reservoir properties. The repeatability focused acquisition design included permanent placement of geophones, making it an ideal candidate for reservoir monitoring.

Time-lapse repeatability was maintained by processing the multiple vintage seismic surveys simultaneously (Lumley et al., 2003) while carefully preserving meaningful information content. In particular, reflection signal from the no-change zones—where time-lapse effects are not expected—was preserved by using nrms as a repeatability metric (Kragh and Christie, 2002). For each main step of the processing, nrms error is measured in the no-change zones and a step is accepted only if its nrms error decreases or is at least maintained from the previous step. This enhancement to the methodology of simultaneous processing makes repeatability monitoring viable throughout the processing sequence rather than at the end with a single reconciliation effort, and thus it alleviates the need for potentially deleterious processes such as cross-equalization of the data after they have been stacked. This processing methodology is discussed in detail by Li et al. (2012).

Following the interpretation of the baseline natural fractures, the reservoir was monitored by the consecutive acquisition of seismic surveys after hydraulic fracturing treatments (Figures 1 and 7). Careful processing of the time-lapse multicomponent data set resulted in higher confidence interpretation within the reservoir interval. The nrms error was found to decrease significantly over that of the former processing, because of the initial treatment of the receiver azimuths preprocessing, which improved the signal-to-noise ratio and the resolved statics (Figure 4). Confidence in the time-lapse anomalies exists only in the areas with the highest repeatability; therefore, the area of interpretation is focused on the polygon section on the nrms map (Figure 4b).

We now turn to the final portion of our discussion of the processing, namely, the prestack shear-wave splitting analysis and layer stripping procedure.

Layer stripping analysis. Shear-wave splitting analysis was conducted on all three vintages of the Pouce Coupe project. We strongly recommend removal of any shear-wave splitting effects from all layers above the reservoir (e.g., via "layer stripping" as in Gaiser, 1999). The reason is straightforward: any shear-wave energy reflected from within the zone of interest must subsequently pass through the layers above it, and thus it arrives at the receivers encoded with all the propagation effects these layers have imposed upon it. Often, as is the case here, the overburden exhibits strong shear-wave splitting, and as such it heavily confounds the information being received from the reservoir.

The shear-wave splitting analysis involves scanning over the full range of trial fast and slow (PS1 and PS2) azimuths. For each azimuth, the data are rotated into the trial PS1, PS2 coordinate system, then a suite of trial time-delays is used

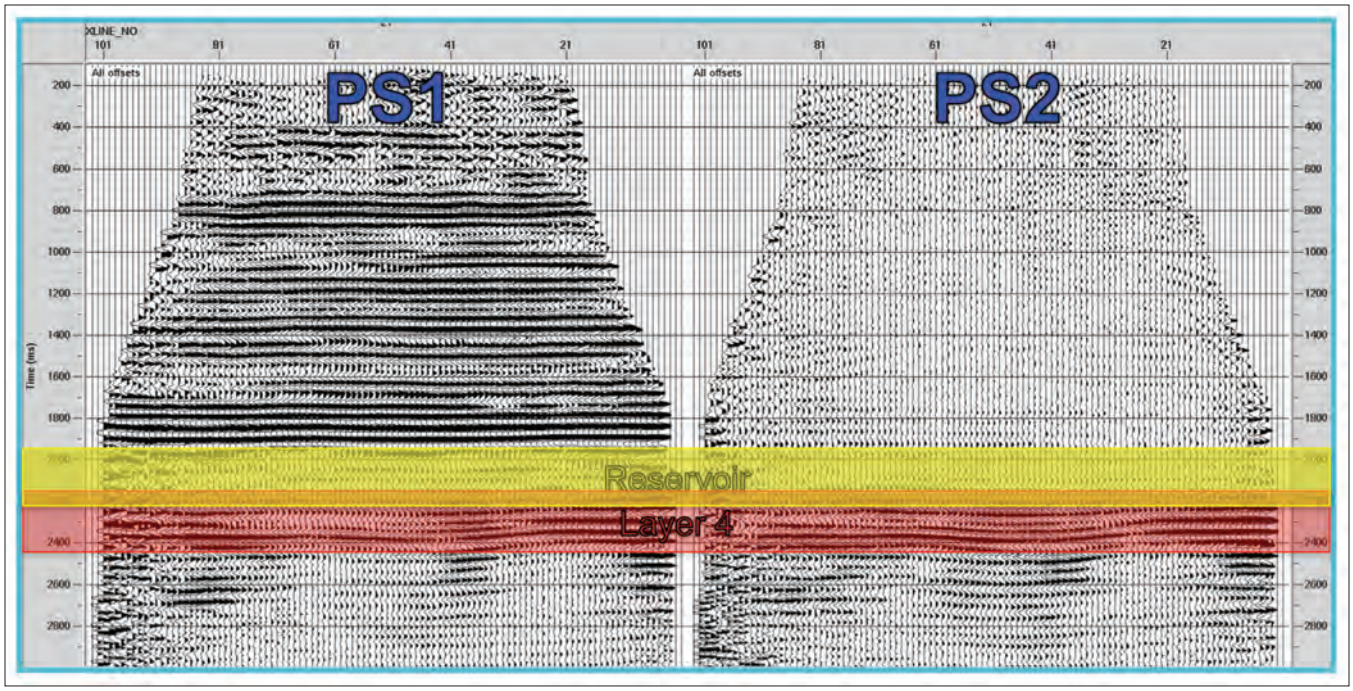

Figure 6. *Final stack result of converted-wave data after processing and layer stripping. The reservoir interval is between 2100 and 2400 ms (outlined in yellow). The final window for the shear-wave splitting analysis is shown by layer 4 (2150–2450 ms).*

to layer-strip the data, and the corresponding suite of results is analyzed upon transformation back to R', T' coordinates. This analysis involves optimization of some sort of objective function (Silver and Chan, 1991); most of the methods currently in use rely on the objective of minimizing the distribution of energy remaining on the transverse component after layer stripping (Li and Grossman, 2012). However, transverse-component-based methods such as these become unstable because of low signal-to-noise ratios, or when only marginal splitting occurs. We have therefore adopted the more sensible radial-component-based objective of maximizing the coherence of the shear-wave energy transferred onto the radial component (Li and Grossman, 2012).

The time-delay and PS1 azimuth estimates resulting from the layer stripping procedure down to the reservoir level are displayed for all three vintages of the Pouce Coupe time-lapse seismic survey in Figure 5. The polygon drawn on each map bounds the area of interest for this study, and the wells are drawn along with hydraulic fracture stages indicated by the small pentagons. The color scale represents the estimated time delays between PS1 and PS2 events while the needle length and orientation represent the estimated PS1 azimuths. Although the maximum estimated time delay is only about 4 ms, which is indeed small, there is, nevertheless, a good correlation between reservoir activity and regions of increasing time delay over the duration of the survey. The PS1 orientation estimates are quite consistent over the duration of the experiment. The significance of these results will be discussed in more detail in the interpretation section.

Montney shale example

The Pouce Coupe time-lapse converted-wave surveys were acquired in 2008 to characterize and monitor changes within the unconventional reservoir caused by hydraulic fracturing. The data set includes a baseline survey acquired after drilling the location's two horizontal northwest-southeast trending wells (2-07 and 7-07), plus two monitor surveys that were obtained subsequent to each of the two corresponding hydraulic fracture treatments (Figure 1). The horizontal wells target the Montney C (2-07) and D (7-07) units of the formation. Because of the proximal location of the field to the Rocky Mountain deformation belt, the stress regime is strongly azimuthally anisotropic, with the maximum horizontal stress being up to 1.8 times the magnitude of the minimum horizontal stress (Davey, 2012). The characteristic tight nature of the Montney unconventional reservoir requires flow pathway heterogeneities, such as natural fractures, to be accessed for economical development.

The fracturing of the reservoir rock creates azimuthally dependent shear strength, and ultimately the shear velocities are different parallel and perpendicular to fracture planes. The use of converted waves for near-vertical fracture interpretation is encouraging because the orientation of the dominant open fractures may be determined and also because the velocity differential (the magnitude of shear-wave azimuthal anisotropy) may provide the ability to characterize fracture density. In comparison, microseismic surveys potentially monitor the volume of reservoir that has reacted to the hydraulic fracture treatment (stimulated reservoir volume), but little is known about how fractures react after proppant is distributed to keep the fracture permeability pathways open, relating to the effective fracture network. This is one application of multicomponent seismic technology where the use of converted waves for imaging reservoir azimuthal anisotropy shows great promise.

The stacked PS1 and PS2 volumes (Figure 6) allow for the

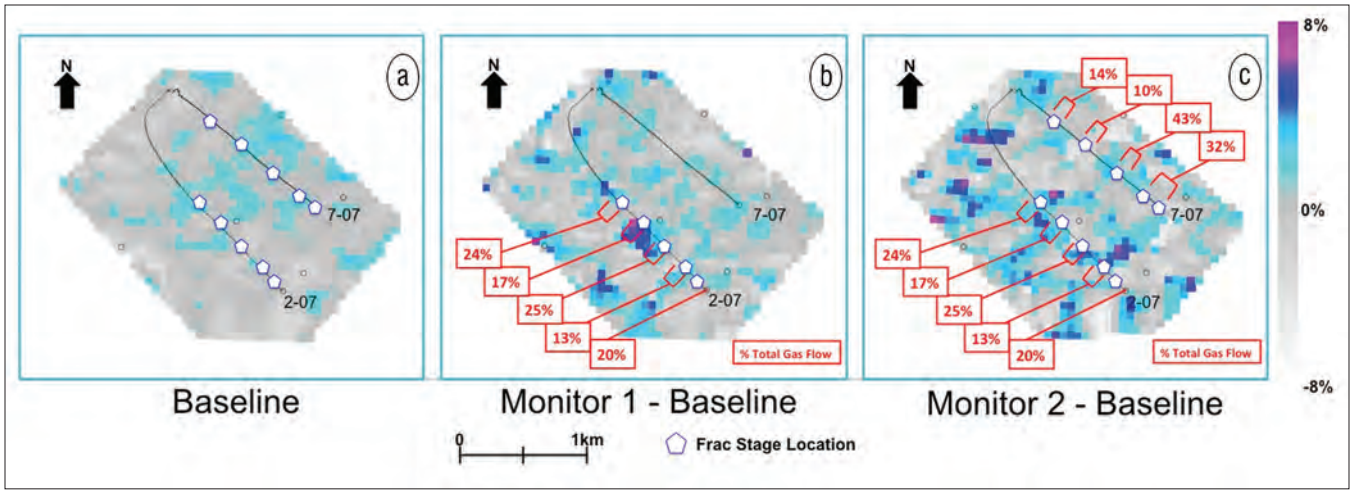

Figure 7. *Map view of the shear-wave splitting averaged over the Montney reservoir interval. Spinner production data are highlighted by frac stage and represented as percentage of total gas flow. (a) Baseline SWVA from shear-wave splitting time-delays. (b) SWVA difference between Monitor 1 and Baseline, after the completion of the 2-07 well. (c) SWVA difference between Monitor 2 and Baseline, after the total completion of 2-07 and 7-07 (hydraulically fractured and propped). Each pixel represents an asymptotic conversion point bin of 50 × 50 m.*

vertical arrival-time differences of the PS1 and PS2 waves to be analyzed within the reservoir more precisely. The poststack approach of estimating the shear-wave velocity anisotropy (SWVA) from shear-wave splitting time-delays is a horizon-based measurement. The SWVA is determined from the difference of travel times between the PS1 and PS2 images of a known seismic marker at the base of the reservoir when there is a lack of coherent reflection energy with the reservoir. This method estimates an effective SWVA anisotropy over the reservoir interval.

A fundamental part of prestimulation unconventional reservoir characterization is determining the natural fracture orientations and their density. The baseline characterization of the SWVA shows low magnitude natural shear-wave azimuthal anisotropy conditions—less than 3% (Figure 7a). The small SWVA values may be caused by nonpreferential orientation of open natural fractures. Although the anomalies are small, the SWVA maps exhibit two main trends orientated northwest and northeast (Figure 7a). Independently, subsurface image log interpretation reveals the Montney Formation has two fracture sets, one orientated parallel to the regional maximum horizontal stress direction (N 40° E) and a perpendicular set (Davey, 2012). Based on the PS1 orientations determined by the layer four shear-wave splitting analysis (Figure 5), it is observed that the principle fast shear-wave orientation varies over the local field scale and may correspond to the two dominant fracture orientations.

Within Pouce Coupe, the fracture set that is likely to fail from hydraulic completions is observed to vary and is controlled by the dominant natural fracture orientation (Davey, 2012). Fracture failure was determined using Mohr-Coulomb failure theory, the treating pressures seen during stimulation, and the variations likely caused by local tectonic reorientations or differential stress cycling history. After the completion of the 2-07 well, three induced SWVA anomalies are present (Figure 7b). The linear induced anomaly (northeast-southwest) at the southern (toe) portion with values between 3 and 5% SWVA may be associated with a wrench fault trending parallel to the present-day regional maximum horizontal stress direction (N40E). This minor offset fault is one of many over the survey area that was only possible to interpret using the converted-wave data. The SWVA anomalies located at the center and heel stages have values between 4 and 7% SWVA and build only south of the well bore representing preferential propagation. The dominant orientation of the highest magnitude anomaly is a result of the hydraulic fracture interacting with the perpendicular natural fracture set (northwest-southeast) and is interpreted as opening fractures against the regional maximum horizontal stress.

Figure 7c shows the overall completion effect of the two horizontal wells. It is believed from the lack of new time-lapse SWVA anomalies near the 7-07 well that the majority of the energy of the completion was lost into the open fractures of a previously interpreted wrench fault, causing the representative SWVA anomaly to grow in size and strength. From the microseismic data analysis (not shown here), it was observed that the microseismic events were focused at the toe of the 7-07 well and propagated toward the 2-07 well, supporting the SWVA results. The other two anomalies near the 2-07 well previously discussed decreased in magnitude and became much more diffuse, representing the equilibrating of reservoir pressure and the fractures closing on the proppant. The dominant fracture orientations did not change between the baseline and monitor surveys (Figure 5), implying that the natural faults and fractures control the displacement of the hydraulic completion energy and the induced anomalies may correspond to propping of pre-existing fracture networks.

The final SWVA signature may reflect the overall connectivity of the open fracture network. It is interesting to compare the shear-wave splitting anomalies with the spinner production data collected for each stage perforation location. In Figure 7b and Figure 7c, the spinner data are portrayed as percent of total gas flow. The percent of total gas production is ultimately related to natural fracture permeability and

hydraulic stimulation success. The baseline fracture locations and density relate to the success of each hydraulic fracture stage and should be used in completion design (Figure 7a). The induced anomalies are related to the ultimate hydrocarbon deliverability and are interpreted to be the propped fractures (Figure 7b and Figure 7c). From multicomponent seismic reservoir characterization and monitoring, the optimum perforation locations can be determined, resulting in an increase of producible gas.

Conclusions

The Pouce Coupe multicomponent time-lapse data provide insight into stress and fracture-related reservoir shear-wave anisotropy through the analysis of shear-wave splitting. The use of converted-wave data to clearly distinguish reservoir anisotropy relied on some key aspects of the processing sequence. We employed novel methods, specifically RADAR to better preserve vector fidelity, nrms-guided simultaneous processing, and coherence of the radial component of the data as objective function for the layer stripping procedure, in our multicomponent processing. This improves prestack shear-wave splitting analysis and layer stripping, and enhances the time-lapse repeatability. We have demonstrated the utility of shear-wave splitting analysis both on common azimuth stacks (stacks over offset only) and poststack (after layer stripping) in determining the SWVA orientation and magnitude by relating these attributes to the "propping" of fractures. TLE

References

Atkinson, J. and T. Davis, 2011, Multicomponent time-lapse monitoring of two hydraulic fracture stimulations in the Pouce Coupe Field unconventional reservoir: First Break, **29**, no. 10, 91–97.

Cary, P., 2002, Detecting false indications of shear-wave splitting: 72nd Annual International Meeting, SEG, Expanded Abstracts, **21**, 1014–1017, http://dx.doi.org/10.1190/1.1816814.

Davey, H., 2012, Geomechanical investigation of the Montney unconventional reservoir, Canada: M.Sc. thesis, Colorado School of Mines.

Gaiser, J., 1999, Applications for vector coordinate systems of 3D converted-wave data: The Leading Edge, **18**, no. 11, 1290–1300, http://dx.doi.org/10.1190/1.1438202.

Grossman, J. P. and R. Couzens, 2012, Preserving converted-wave vector fidelity with an automated receiver-azimuth detection algorithm: The Recorder, **37**, no. 7 (November 2012).

Martin, M. and T. Davis, 1987, Shear-wave birefringence: A new tool for evaluating fractured reservoirs: The Leading Edge, **6**, no. 10, 22–28, http://dx.doi.org/10.1190/1.1439333.

Kragh, E. and P. Christie, 2002, Seismic repeatability, normalized rms, and predictability: The Leading Edge, **21**, no. 7, 640–647, http://dx.doi.org/10.1190/1.1497316.

Li, X., R. Couzens, J. P. Grossman, and K. Lazorko, 2012, Simultaneous time-lapse processing for improved repeatability: First Break, **30**, 107–110.

Li, X. and J. P. Grossman, 2012, A stable criterion for shear-wave-splitting analysis: GeoConvention 2012: Vision, Expanded Abstracts.

Lumley, D., D. C. Adams, M. Meadows, S. Cole, and R. Wright, 2003, 4D seismic data processing issues and examples: 73rd Annual International Meeting, SEG, Expanded Abstracts, 1394–1397, http://dx.doi.org/10.1190/1.1817550.

Silver, P. G., and W. W. Chan, 1991, Shear wave splitting and subcontinental mantle deformation: Journal of Geophysical Research, **96**, B10, 16,429–16,454, http://dx.doi.org/10.1029/91JB00899.

Acknowledgments: We thank Talisman Energy (especially David D'Amico, Eric Andersen, and Heath Pelletier) for their review and permission to show the processing results. We also thank Rodney Couzens for processing, review, and helpful discussions, Colorado School of Mines, Tom Davis for his leadership and helpful guidance, and Heather Davey, David Cho, and Bonnie Nasim for proofreading.

Corresponding author: jeff_grossman@sensorgeo.com